



## Relation between Self-Diffusion and Viscosity in Dense Liquids: New Experimental Results from Electrostatic Levitation

J. Brillo,\* A. I. Pommrich, and A. Meyer

*Institut für Materialphysik im Weltraum, Deutsches Zentrum für Luft- und Raumfahrt (DLR), 51170 Köln, Germany*

(Received 20 July 2011; published 10 October 2011)

By using the technique of electrostatic levitation, the Ni self-diffusion, density, and viscosity of liquid  $Zr_{64}Ni_{36}$  have been measured *in situ* with high precision and accuracy. The inverse of the viscosity,  $\eta$ , measured via the oscillating drop technique, and the self-diffusion coefficient  $D$ , obtained from quasielastic neutron scattering experiments, exhibit the same temperature dependence over 1.5 orders of magnitude and in a broad temperature range spanning more than 800 K. It was found that  $D\eta = \text{const}$  for the entire temperature range, contradicting the Stokes-Einstein relation.

DOI: 10.1103/PhysRevLett.107.165902

PACS numbers: 66.10.cg, 66.20.Gd

The dynamics in fluids is governed by two intimately related properties: viscosity and atomic diffusion. While the first describes the macroscopic transport of momentum by the collective motion of the particles, the latter describes single-particle diffusive transport. A common relation, which is often taken for granted in order to calculate the required diffusion coefficients of atoms or molecules in a liquid from the viscosity, or vice versa, is the Stokes-Einstein relation [1]:

$$D\eta = \frac{k_B T}{6\pi r_H} \quad (1)$$

In Eq. (1),  $\eta$  is the viscosity of the solvent,  $D$  is the diffusion coefficient,  $r_H$  is its hydrodynamic radius,  $T$  is the absolute temperature, and  $k_B = 1.38 \times 10^{-23}$  J/K is the Boltzmann constant. The Stokes-Einstein relation was derived in order to study the diffusive motion of a mesoscopic sphere in a viscous medium [2]. However, when the diffusing objects are of atomistic size, deviations of  $D$  and  $\eta$  from the Stokes-Einstein behavior can be observed.

For instance, molecular dynamics simulations, performed on liquid  $Al_{80}Ni_{20}$ , show that Eq. (1) works as a good approximation when  $T$  is extremely large ( $T \geq 1800$  K) and becomes increasingly inaccurate upon lowering  $T$  below this temperature [3]. The same is indicated for  $ZrCu_2$  [4], various Lennard-Jones [5–7] and hard-sphere systems [8], water [9], and silica [10]. For the latter system,  $\eta$  and  $D$  deviate from Eq. (1) over the entire investigated temperature range.

Experimental indications for a deviation from Eq. (1) exist for some liquid metals [11,12] and for molecular glass-forming liquids [13].

On a large scale, however, Eq. (1) is at least a good approximation: For instance, in the case of PdNiCuP [14], Pd self-diffusion and viscosity have been measured over a temperature range from 600 to 1200 K. Both properties vary by 10 orders of magnitude. Equation (1) worked within a factor of 2.

From an experimental point of view, a direct proof of Eq. (1) is still very difficult due to the lack of reliable experimental data, especially of the transport coefficients  $D$  and  $\eta$ . The accurate measurement of diffusion data, using long capillary methods, is subject to large errors due to additional transport of mass by buoyancy-driven flow effects [15,16]. Pollution of the sample from chemical reactions with the container walls complicates the measurement of both properties. In order to check Eq. (1), measurements need to be carried out over a sufficiently large temperature range in which  $T$  changes by a factor of 1.5–2. This includes high temperatures favoring convection and chemical reactivity.

With the development of advanced containerless processing techniques, such as electrostatic levitation (ESL), we are now in a position to master these challenges.

Using ESL, we recently carried out quasielastic neutron scattering experiments and determined accurate Ni self-diffusion coefficients  $D_{Ni}$  in liquid  $Zr_{64}Ni_{36}$ . These data were measured over a broad temperature range from 1100 to 1700 K [17]. The viscosity and density of liquid  $Zr_{64}Ni_{36}$  were also measured over a broad temperature range:  $T$  varied by a factor of 1.5, whereas the viscosity varied by 1.5 orders of magnitude. With these results for a dense glass-forming system, we can now check the relation of viscous flow and diffusion of mass in unequaled detail.

Previous density and viscosity data of  $Zr_{64}Ni_{36}$  have been published by Ohsaka, Chung, and Rhim [18]. In contrast to these works, our own electrostatic levitator is equipped with a more advanced sample-positioning system as well as a sophisticated optical setup, using a high-speed camera. The use of the latter is new for the measurement of the viscosity in electrostatic levitation. It allows us to determine the droplet radii with a high precision, thus increasing the overall accuracy of the data.

Experiments in ESL are carried out under  $\approx 10^{-8}$  mbar. The electrically charged samples have typical diameters between 1.5 and 3 mm and masses of 20–90 mg. A sample is levitated in the static electric field between two parallel

disklike electrodes 15 mm apart from each other. Horizontal stabilization is accomplished by four lateral electrodes underneath the sample. Position control is achieved from a feedback loop consisting of two expanded He/Ne lasers arranged perpendicular to each other and associated  $x$ - and  $y$ -position sensitive detectors.

Heating and melting of the specimen are achieved by two 25 W IR lasers. Temperature gradients, eventually generated this way, are so small that they can be neglected [17]. Temperature is measured by a pyrometer directed at the specimen from the side. As the effective emissivity is generally not known, it has to be calculated from the known liquidus temperature under the reasonable assumption that it is constant over the entire investigated temperature range. The liquidus temperature  $T_L = 1283$  K is used from the phase diagram [19]. In all experiments, the observed mass losses were lower than 0.1% of the original mass. Density is measured by illuminating the sample from one side by a cold light source and recording shadow images by means of a digital complementary metal-oxide-semiconductor camera with a resolution of  $480 \times 500$  pixel and a frame rate of 2000 Hz. The images are analyzed, and the sample volume  $V$  is calculated from the edge curves. The density is obtained with a precision of better than  $\Delta\rho/\rho < 0.5\%$ . The duration of a complete measurement cycle was approximately 10 s.

The viscosity is measured by using the same optical setup. A sinusoidal electric field with an amplitude of 0.4–2 kV is superimposed onto the vertical electrodes with a frequency between 100 and 400 Hz. When the excited  $P_{2,0}$  mode has stabilized with an amplitude of 4% of the quiescent droplet radius  $R_0$ , the sinusoidal field is switched off and the sample oscillates freely. During the decay of the oscillation, shadow graphs of the sample are recorded.

The use of a high-speed camera allows us to collect 10–20 data points per oscillation and to determine the vertical radius  $R_z(t)$  as a function of time  $t$  with a precision of better than 1%. For the viscosity measurement, the duration of an experimental run was roughly 15 min. Figure 1 shows  $R_z(t)$  for a measurement at 1182 K. For further analysis,  $R_z(t)$  is fitted by a damped sine function:  $R_z(t) = R_0 + A \exp(-\frac{t}{\tau_0}) \sin(\omega t + \delta_0)$ , where  $A$  is the amplitude,  $\tau_0$  is the decay time constant,  $\omega$  is the frequency, and  $\delta_0$  is the constant phase shift. From the obtained value of  $\tau_0$ , the viscosity is calculated according to Lamb's law [20]:

$$\eta = \frac{\rho R_0^2}{5\tau_0}. \quad (2)$$

Density data were obtained over a broad temperature range. An undercooling of nearly 180 K is achieved. The scatter of the data is smaller than 0.1%, and the agreement among different experimental runs, as well as with Ref. [18], is within  $\pm 0.15\%$ .

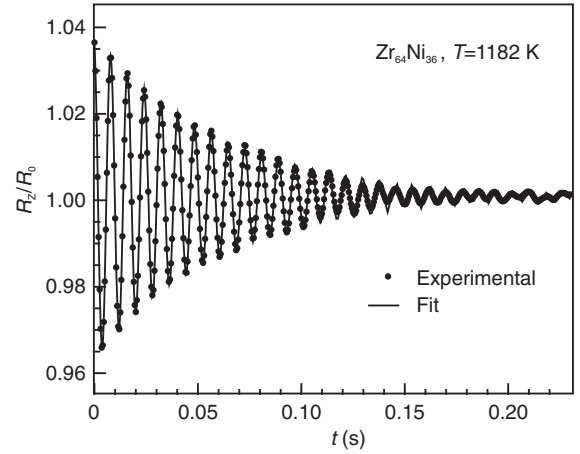


FIG. 1. Vertical radius  $R_z$  versus time  $t$  measured at 1182 K during the decay of the oscillation (symbols). The solid line is a fit of a damped sine law.

The density can be expressed by a linear law with  $\rho_L = 6.878 \pm 0.003$  g  $\cdot$  cm $^{-3}$  being the density at liquidus temperature  $T_L$  and  $\rho_T = -3.73 \pm 0.01 \times 10^{-4}$  g  $\cdot$  cm $^{-3}$  K $^{-1}$  the temperature coefficient.  $\rho_L$  corresponds to a mean particle density of  $\hat{\rho} = 0.052$  at/ $\text{\AA}^3$ . By using the covalent radii of Zr and Ni,  $r_{\text{Zr}} = 1.45$   $\text{\AA}$  and  $r_{\text{Ni}} = 1.15$   $\text{\AA}$  [21], respectively, a value of  $0.55 \pm 0.002$  is obtained for the effective volume packing fraction:  $\varphi = \frac{4\pi}{3} \times (0.36r_{\text{Ni}}^3 + 0.64r_{\text{Zr}}^3)\hat{\rho}$ . This value is in line with  $\varphi$  from multicomponent bulk glass-forming alloys [12]. As for comparison, the packing fraction of liquid Al is  $\approx 0.48$ . Hence,  $\text{Zr}_{64}\text{Ni}_{36}$  is a rather densely packed system, and glassy behavior should be favored already at this stage.

Results of the viscosity measurement are shown in Fig. 2 as a function of temperature. Values were obtained in the broad temperature range of 1050–1750 K. Large undercoolings of up to 230 K were achieved. Generally, the viscosity increases when the temperature is lowered. At  $T_L$ , the viscosity is 11.5 mPa  $\cdot$  s. It reaches a value of approximately 130 mPa  $\cdot$  s for  $T \approx 1100$  K which is large compared to most non-glass-forming metallic alloys, [22]. For  $T > T_L$ ,  $\eta$  assumes values between 11.5 and 8 mPa  $\cdot$  s.

In Fig. 2, the data are shown together with the viscosities of Ohsaka, Chung, and Rhim [18]. For  $T < T_L$ , there is an agreement within  $\pm 5\%$  corresponding to the scatter of our data. For  $T > T_L$ , however, the two curves significantly deviate from each other. This deviation increases with an increase of temperature. At 1500 K, the viscosity reported by Ohsaka, Chung, and Rhim [18] is about 30% smaller.

In order to exclude that this discrepancy is caused by a systematic error in our data, due to some nonlinear effect in the surface oscillation, the experiment was performed with five samples having masses of 20.8, 27.0, 38.2, 41.0, and 86.2 mg. Such a nonlinear effect could originate, for instance, from an excitation of flow vortices in the bulk of the droplet when the oscillation amplitude is too large [23].

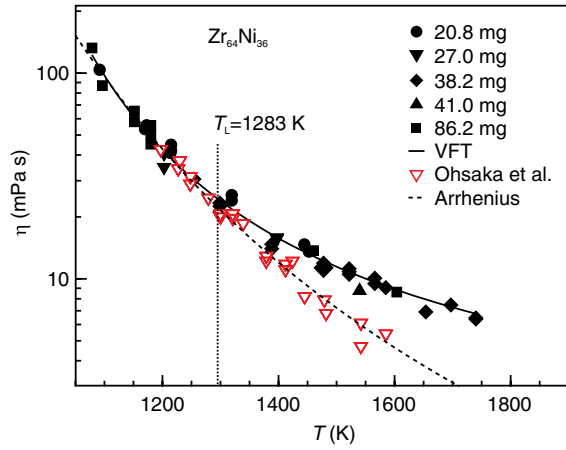


FIG. 2 (color online). Viscosity of  $Zr_{64}Ni_{36}$  as a function of temperature. The solid symbols correspond to data obtained from samples with different masses and the solid line a corresponding fit of the Vogel-Fulcher-Tammann law, Eq. (3). Shown for comparison are data from Ohsaka, Chung, and Rhim [18] (open symbols) with a corresponding fit of an Arrhenius law (dashed line).

Recently, Ishikawa *et al.* argued [24] that there is an interference of the surface oscillation by the positioning controller which would also lead to an apparently increased viscosity. In case such a nonlinear effect existed in the droplet oscillation, using samples with different masses would result in apparently different values of the viscosity. As shown in Fig. 2, however, the same curve  $\eta(T)$  is obtained for each sample mass within the above mentioned  $\pm 5\%$  scatter. Systematic errors due to nonlinear droplet oscillations can, hence, be excluded.

Our data can well be described by the phenomenological Vogel-Fulcher-Tammann (VFT) law, which is typical for many glass-forming systems [25]:

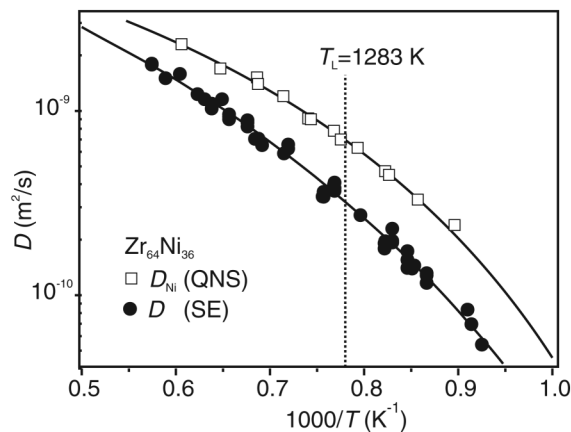


FIG. 3. Diffusion constants versus inverse temperature. The circles represent  $D_\eta$  obtained from  $\eta$  via the Stokes-Einstein relation, Eq. (1). The squares correspond to the Ni self-diffusion constant  $D_{Ni}$ , directly measured by quasielastic neutron scattering. Corresponding fits of the VFT law are shown by solid lines.

$$\eta = \eta_0 \exp\left(\frac{E_\eta}{k_B(T - T_0)}\right). \quad (3)$$

In this equation, the constant  $E_\eta$  corresponds to an activation energy for viscous flow,  $T_0$  describes a temperature associated with the glass transition, and  $\eta_0$  is a scaling factor. Equation (3) reproduces the measured data with parameters obtained from the fit as  $E_\eta = 2.75 \times 10^{-20}$  J,  $T_0 = 660.5$  K, and  $\eta_0 = 1.1$  m · Pa · s; see Fig. 2.

Our Ni self-diffusion coefficients  $D_{Ni}$  are plotted semi-logarithmically in Fig. 3 against the inverse temperature. The uncertainty of  $D_{Ni}$  is of the order of  $\pm 5\%$  only, and values range from  $2.3 \times 10^{-9}$  m<sup>2</sup> s<sup>-1</sup> at  $T \approx 1650$  K to  $2.3 \times 10^{-10}$  m<sup>2</sup> s<sup>-1</sup> at  $\approx 1116$  K, corresponding to an undercooling of 167 K. At liquidus temperature  $T_L = 1283$  K,  $D_{Ni} = 7.8 \times 10^{-10}$  m<sup>2</sup> s<sup>-1</sup>.

A VFT law, similar to Eq. (3), can be fitted to these data as well. Apart from the scaling factor, absolute values obtained for the activation energy  $E_D = -2.64 \times 10^{-20}$  J and for the temperature  $T_0 = 674$  K are identical within error bars to the corresponding values obtained from the viscosity data. Moreover,  $E_D \approx -E_\eta$ . Hence, both the inverse of the viscosity, i.e.,  $\eta^{-1}$ , and the self-diffusion coefficient are proportional to each other. This is shown in Fig. 4, where the measured viscosity data are multiplied by the VFT fit of  $D_{Ni}$ : The product  $D_{Ni}\eta$  equals  $1.8(\pm 0.25) \times 10^{-11}$  J/m over the entire temperature range of  $1050$  K  $\leq T \leq 1750$  K.

For comparison, Fig. 4 shows the Stokes-Einstein relation with the hydrodynamic radius  $r_H$  being set to  $r_{Ni} = 1.15$  Å. The experimental data are underestimated by more than a factor of 2, and the temperature dependence is significantly different: While from experiment  $D_{Ni}\eta = \text{const}$  is found,  $D_{Ni}\eta$  scales with  $k_B T$  in Eq. (1). This is

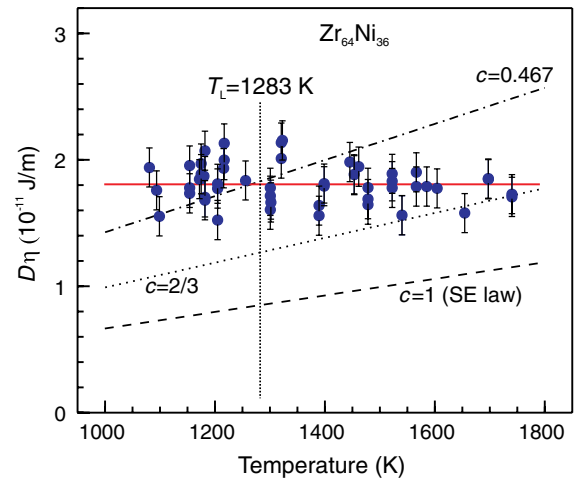


FIG. 4 (color online).  $D_{Ni} \cdot \eta$  versus temperature (symbols). In order to guide the eye, a linear fit to the data is also shown (solid line). The dashed and dotted lines correspond to the Stokes-Einstein relation, Eq. (1), with different choices of the hydrodynamic radius  $r_H = cr_{Ni}$ .

also evident from Fig. 3, where  $D$ , calculated from  $\eta$ , is also shown. The measured self-diffusion coefficients  $D_{\text{Ni}}$  are underestimated by more than 70%, and the significantly different temperature dependence in Fig. 3 is already visible by the eye.

In an attempt to better fit Eq. (1) to the experimental data, the hydrodynamic radius  $r_{\text{H}}$  is set to  $c r_{\text{Ni}}$  with  $c$  being a coefficient. With  $c = 2/3$ , Eq. (1) transforms into the Sutherland-Einstein relation [26]. If  $c = 0.467$ , Eq. (1) matches the experimental data at least at  $T_{\text{L}}$ . In this case,  $r_{\text{H}} \approx 0.53 \text{ \AA}$ . However, the agreement among the temperature dependencies becomes even worse when  $r_{\text{H}}$  is lowered; see Fig. 4. This could be resolved only by the use of a temperature-dependent radius. In this case,  $r_{\text{H}}$  would have to vary by a physically unrealistic factor of 1.7 over the investigated temperature range.

According to mode-coupling theory [27], the dynamics in a liquid is strongly coupled when the particle density is large. This leads to a freezing of the atomic motion when a critical temperature  $T_c$  is approached upon cooling. In this case, the diffusion coefficient  $D$  and the inverse of the viscosity,  $\eta^{-1}$ , are proportional to the same scaling law  $(T - T_c)^\gamma$  with  $\gamma > 0$  being a nonuniversal exponent. Hence, when  $T \rightarrow T_c$ ,  $D\eta = \text{const}$  is asymptotically obtained. From a comparison to dynamics in multicomponent Zr-based bulk glass-forming alloys [28],  $T_c$  is estimated to be  $\approx 900 \text{ K}$  in  $\text{Zr}_{64}\text{Ni}_{36}$ . Our results have been obtained at temperatures well above  $T_c$ . Apparently, possible deviations from the mode-coupling-theory scaling behavior are similar with respect to temperature for both mass transport coefficients.

In conclusion, by using ESL as an advanced technique, the quality of the obtained experimental data allowed us to establish a relation between viscosity and self-diffusion in the case of  $\text{Zr}_{64}\text{Ni}_{36}$ . We find  $D\eta = \text{const}$ , which is in line with mode-coupling-theory predictions for temperatures close to  $T_c$  but in contrast to the Stokes-Einstein relation. Whether this is also valid for a less dense liquid,  $\varphi < 0.5$ , is a subject of ongoing research.

We thank Thomas Voigtmann and Matthias Sperl for a critical reading of the manuscript.

---

\*juergen.brillo@dlr.de

- [1] A. Einstein, *Investigation on the Theory of the Brownian Movement* (Dover, New York, 1926).  
 [2] A. Einstein, *Ann. Phys. (Leipzig)* **322**, 549 (1905).

- [3] S. K. Das, J. Horbach, and T. Voigtmann, *Phys. Rev. B* **78**, 064208 (2008).  
 [4] X. J. Han and H. R. Schober, *Phys. Rev. B* **83**, 224201 (2011).  
 [5] F. Affouard, M. Descamps, L. C. Valdes, J. Habasaki, P. Bordat, and K. L. Ngai, *J. Chem. Phys.* **131**, 104510 (2009).  
 [6] P. Bordat, F. Affouard, M. Descamps, and F. Müller-Plathe, *J. Phys. Condens. Matter*, **15**, 5397 (2003).  
 [7] W. Kob and H. C. Andersen, *Phys. Rev. E* **51**, 4626 (1995).  
 [8] S. K. Kumar, G. Szamel, and J. F. Douglas, *J. Chem. Phys.* **124**, 214501 (2006).  
 [9] S. R. Becker, P. H. Poole, and F. W. Starr, *Phys. Rev. Lett.* **97**, 055901 (2006).  
 [10] J. Horbach and W. Kob, *Phys. Rev. B* **60**, 3169 (1999).  
 [11] J. Brillo, S. M. Chathoth, M. M. Koza, and A. Meyer, *Appl. Phys. Lett.* **93**, 121905 (2008).  
 [12] A. Meyer, W. Petry, M. Koza, and M.-P. Macht, *Appl. Phys. Lett.* **83**, 3894 (2003).  
 [13] H. Sillescu, *J. Non-Cryst. Solids* **243**, 81 (1999).  
 [14] A. Bartsch, K. Rätzke, A. Meyer, and F. Faupel, *Phys. Rev. Lett.* **104**, 195901 (2010).  
 [15] A. Meyer, *Phys. Rev. B* **81**, 012102 (2010).  
 [16] B. Zhang, A. Griesche, and A. Meyer, *Phys. Rev. Lett.* **104**, 035902 (2010).  
 [17] T. Kordel, D. Holland-Moritz, F. Yang, J. Peters, T. Unruh, T. Hansen, and A. Meyer, *Phys. Rev. B* **83**, 104205 (2011).  
 [18] K. Ohsaka, S. K. Chung, and W. K. Rhim, *Acta Mater.* **46**, 4535 (1998).  
 [19] T. B. Massalski, *Binary Alloy Phase Diagrams* (American Society for Metals, Materials Park, OH, 1996).  
 [20] H. Lamb, *Hydrodynamics* (Cambridge University Press, Cambridge, England, 1993), 6th ed.  
 [21] L. Pauling, *J. Am. Chem. Soc.* **69**, 542 (1947).  
 [22] K. C. Mills, *Recommended Values of Thermophysical Properties for Selected Commercial Alloys* (Woodhead, Cambridge, England, 2002).  
 [23] E. Becker, W. J. Hiller, and T. A. Kowalewski, *J. Fluid Mech.* **258**, 191 (1994).  
 [24] T. Ishikawa, P.-F. Paradis, N. Koike, and Y. Watanabe, *Rev. Sci. Instrum.* **80**, 013906 (2009).  
 [25] K. Binder and W. Kob, *Glassy Materials and Disordered Solids, An Introduction to Their Statistical Mechanics* (World Scientific, Singapore, 2005).  
 [26] W. Sutherland, *Philos. Mag.* **9**, 781 (1905).  
 [27] W. Götze, in *Liquids, Freezing and the Glass Transition*, Proceedings of the Les Houches Summer School of Theoretical Physics, Session LI, edited by J.-P. Hansen, D. Levesque, and J. Zinn-Justin (North-Holland, Amsterdam, 1991), p. 287.  
 [28] T. Voigtmann, A. Meyer, D. Holland-Moritz, S. Stüber, T. Hansen, and T. Unruh, *Europhys. Lett.* **82**, 66001 (2008).